A Semi-Microscopic Monte Carlo Study of Permeation Energetics in a Gramicidin-Like Channel: The Origin of Cation Selectivity

Vladimir Dorman, Michael B. Partenskii, and Peter C. Jordan
Department of Chemistry, Brandeis University, Waltham, Massachusetts 02254-9110 USA

ABSTRACT The influence of a gramicidin-like channel former on ion free energy barriers is studied using Monte Carlo simulation. The model explicitly describes the ion, the water dipoles, and the peptide carbonyls; the remaining degrees of freedom, bulk electrolyte, non-polar lipid and peptide regions, and electronic (high frequency) permittivity, are treated in continuum terms. Contributions of the channel waters and peptide COs are studied both separately and collectively. We found that if constrained to their original orientations, the COs substantially increase the cationic permeation free energy; with or without water present, CO reorientation is crucial for ion-CO interaction to lower cation free energy barriers; the translocation free energy profiles for potassium-, rubidium-, and cesium-like cations exhibit no broad barriers; the lipid-bound peptide interacts more effectively with anions than cations; anionic translocation free energy profiles exhibit well defined maxima. Using experimental data to estimate transfer free energies of ions and water from bulk electrolyte to a non-polar dielectric (continuum lipid), we found reasonable ion permeation profiles; cations bind and permeate, whereas anions cannot enter the channel. Cation selectivity arises because, for ions of the same size and charge, anions bind hydration water more strongly.

INTRODUCTION

In a series of papers we have pursued a semimicroscopic (SMC) approach to modeling the free energy of ion permeation through single file ion channels (Partenskii et al., 1991a,b; Partenskii and Jordan, 1992a,b; Partenskii et al., 1994; Sancho et al., 1995). We introduced this method to provide a bridge between[1] simple continuum electrostatic models and the far more complex "realistic" molecular dynamics (MD) treatment. In this way we could retain the simplicity of the continuum approach without being limited by its unrealistic assumptions about the dielectric properties of the selectivity domains of ion channels. Here we focus on gramicidin. The purpose of our simplification is to consider individually and collectively the influence that pore water, the backbone carbonyls, the lipid, and bulk water have on permeation. We indicate how the approach can be extended to include the remaining backbone moieties and the peptide's polar side chains.

Gramicidin remains a uniquely attractive system for theoretical study. The peptide backbone structure of the predominant electrically active membrane bound form is known (Nicholson and Cross, 1989), and there is strong evidence establishing the alignment of the polar tryptophan side chains (Ketchem et al., 1993). There is a wealth of experimental data characterizing ion interaction with the channel (for a recent review, see Andersen and Koeppe, 1992). Whereas there remain uncertainties with respect to the location of the side chains, it is possible to construct reasonable initial structures as a basis for understanding the origin of the channel's selectivity. The consensus description of monovalent cation permeation is that in gramicidin A the ion binds near the channel mouth, and that exiting the channel, not translocation, is rate limiting (Andersen, 1983; Eisenman and Sandblom, 1984; Jakobsson and Chiu, 1987). Monovalent anions neither permeate nor block even though the channel is large enough to permit the entry of the smaller halides. Theoretical work, based on MD (Roux and Karplus, 1993) yields a permeation profile for Na^+ that is consistent with important experimentally observed features, in particular the location of the univalent cation binding site (Olah et al., 1991). However, the associated free energy profile, although qualitatively reasonable, exaggerates both wells and barriers. Studies on the other alkali cations yield similar results (Roux et al., 1995). An alternate approach, the application of the protein dipole-Langerin dipole method (Warshel and Russell, 1984), justified by free energy perturbation calculations (Åqvist and Warshel, 1989; Lee et al., 1993), yields a Na^+ free energy profile that is more reasonable energetically but places the binding site too close to the channel exit (Åqvist and Warshel, 1989). There are competing explanations for the channel's valence selectivity (Urry et al., 1981; Sung and Jordan, 1987b), but this question remains unresolved. Here we investigate the permeation energetics of the alkali cations Cs^+, Rb^+, and K^+, and the halides Cl^- and F^- to determine if we can recover major features of the cationic free energy profiles and to establish why gramicidin A, in which there is no obvious mechanism for polarity discrimination, is ideally valence selective.

SMC models explicitly describe a limited set of molecular degrees of freedom, e.g., the rotation of the water dipoles in the channel (Partenskii et al., 1991a,b; Partenskii and Jordan, 1992a,b; Sancho et al., 1995), the reorientation of those polar groups of the channel forming protein lining the permeation pathway (Partenskii and Jordan, 1992b; Partenskii et al., 1994), etc. A semicontinuum approach is

Received for publication 12 June 1995 and in final form 4 October 1995.
Address reprint requests to Dr. Peter C. Jordan, Department of Chemistry, Brandeis University, Waltham, MA. 02254-9110. Tel.: 617-736-2540; Fax: 617-736-2516; E-mail: jordan@binah.cc.brandeis.edu.

0006-3495/96/01/121/14 $2.00

used to describe the high frequency polarizability of the channel water molecules, the channel former and the lipid; bulk solvent is described as a macroscopic continuum dielectric (for discussion see Partenskii et al., 1994). Whereas it is much more detailed in its treatment of interparticle interactions, the MD approach, when used for studying the energetics of permeation through lipid bound single file channels, gives rise to significant uncertainties. The computational potentials, having been optimized to describe solvation in bulk water with its open network structure (Berendsen et al., 1981, 1987; Jorgensen et al., 1983), are of uncertain reliability in the vastly different solvation environment of a narrow channel. Calculations on gramicidin indicate that standard computational potentials must be significantly modified if they are to properly account for cation binding to gramicidin (Roux and Karplus, 1993; Roux et al., 1995). MD calculations are extremely computer intensive; systematic variation of the parameters of the potential function to determine their effect on permeation energetics and to establish what range of parameters are physically reasonable is out of the question. Furthermore, MD requires cutting off the long-range electrostatic interactions, an approximation requiring careful handling of electrostatic boundary conditions (Lee et al., 1993), lest further inaccuracies are introduced.

The SMC approach has more limited goals than MD and cannot provide the wealth of molecular detail. However, because it focuses on a restricted set of dynamical variables, determining the free energy profile for an ion in the channel does not make large computational demands. Instead of the time consuming process of umbrella sampling followed by melding of potential of mean force segments (Pangali et al., 1979), we directly computed the free energy at each position of the ion. It was then possible to vary the model parameters and analyze their effect on the permeation free energy, and to rapidly carry out perturbative studies. Furthermore, our implementation of the SMC approach permitted exact treatment of all long range electrostatic interactions, thus avoiding any problems because of electrostatic boundary conditions. Our method is an improvement over macroscopic continuum models because we made no unrealistic (and untestable) assumptions about the dielectric properties of the different structural regions (Partenskii and Jordan, 1992a; Partenskii et al., 1994). Finally, we can readily investigate the influence that variation of the potential function and its parameters has on the free energy profile.

The basic SMC model of a single file (gramicidin-like) channel, devised to test the hypothesis that channel water forms a high dielectric constant domain (Partenskii et al., 1991a), is a linear chain comprising the ion and a limited number of water molecules embedded in a continuum dielectric slab (Partenskii and Jordan, 1992b). The latter accounts for the dielectric influence of the lipid and, in an approximate way, for the high frequency dielectric polarizability of waters and of the channel forming peptide. The whole ensemble is sandwiched between continuum dielectrics descriptive of bulk water. In addition, there is a narrow transitional region between bulk water and membrane (analogous to the "Helmholtz layer" (Bockris and Reddy, 1977)).

Our earlier studies of this model have shown that water in single file channels is strongly polarized by an ion at any site in the channel, and that the effective dielectric constant of the pore water, $\epsilon_{eff} \sim 3 - 5$ (Partenskii and Jordan, 1992b), is much lower than the bulk value (~ 80) assigned in most continuum modeling (Parsegian, 1969; Levitt, 1978; Jordan, 1984; Jordan et al., 1989; Monoi, 1991). The approach has been generalized to study cation selectivity (Sancho et al., 1995). When applied to gramicidin, the results are consistent with known translocational selectivity (Urban et al., 1980; Andersen, 1983). Other SMC studies have treated the influence of the polar groups lining gramicidin's interior (the carbonyls) in an oversimplified manner. To maintain cylindrical symmetry, thus facilitating statistical mechanical analysis, the helical distribution of the channel carbonyls was approximated by distributing the COs on rings. This procedure, although demonstrating the stabilizing influence of the peptide, led to significant overestimates of the variation of the free energy profile in the channel (Partenskii et al., 1994).

Whereas chemical mutagenesis has demonstrated that the side chains affect permeation in gramicidin (for reviews, see (Killian, 1992; Andersen and Koeppe, 1992; Busath, 1993)), the dominant interaction is between the ion and the peptide backbone, which continues to be the focus of our study. Here we relax the restriction that localized the CO groups to rings and properly account for gramicidin's helical structure, including libration of the COs. Both amines and carbonyls of the peptide backbone interact with the permeant ion. However, the CO bond is longer and more polar (it is the major contributor to the peptide dipole); we thus assume that ion-carbonyl interaction is the main influence on the interaction between the ion and gramicidin. The permeation free energy relative to bulk water is calculated by means of a multi-step thermodynamic exchange process: the transfer of an ion from bulk water to vacuum (the "dehydration process") and the complementary transfer of a water molecule from vacuum to bulk water; the transfer of the ion from vacuum to a uniform dielectric with $\epsilon = \epsilon_{background}$ and the transfer of a water molecule in the opposite direction; the exchange of a water molecule residing at some site in the channel for the ion in the uniform dielectric background (this gives rise to a stabilization free energy attributable to interaction of the ion with the water chain, gramicidin's carbonyl groups, the lipid and bulk water).

Calculation of the stabilization free energy is done using the Monte Carlo (MC) method. We considered a number of ways of estimating the other terms using both experimental data and theoretical models. We show that, taken together, these contributions lead to low affinity cation binding by the channel, consistent with high permeation rates. In contrast, for an anion of the same radius and charge density, there is a significant barrier to ion entry, which accounts for the fact that anions do not

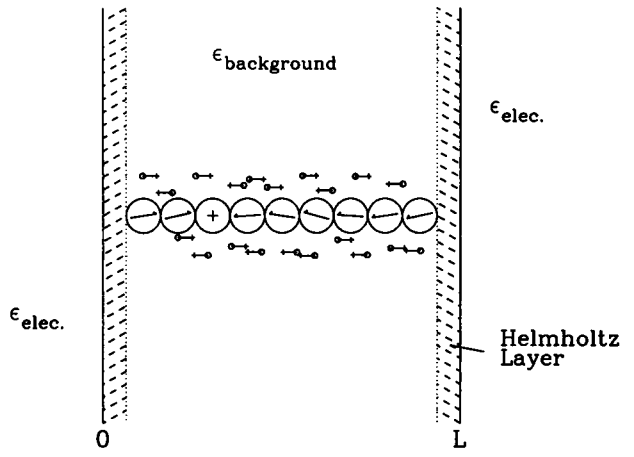

FIGURE 1 Semi-microscopic model of the ion-water-channel-lipid-electrolyte ensemble. A Helmholtz layer, which accounts for orientationally ordered bulk water, is included. The region between 0 and L forms the background dielectric. The external regions contain electrolyte in which $\epsilon_{elec.} \sim \infty$ (see text). The water dipoles are aligned by the ion, located at site 3 in this diagram. Surrounding the ion-water chain is a planar projection of part of gramicidin's native carbonyl distribution (carbonyl reorientation due to interaction with the ion is not illustrated); to avoid confusion, only 20 of the 32 COs are depicted. The carbon atoms are designated (+) and the oxygen atoms (O).

appear to interact with gramicidin, neither permeating nor blocking. An obvious rationale for this effect is the asymmetry of water molecules; see Verwey, 1942; Buckingham, 1957; Straatsma and Berendsen, 1988; Jayaram et al., 1989; Roux et al., 1990; Hirata et al., 1988 and references therein. This point is illustrated using simple estimates. Finally, we note that polarity dependent differences in dehydration energy may be a recurring motif that can have significant influence on channel function generally.

MODEL AND BASIC EQUATIONS

The computational model is illustrated in Fig. 1. Streaming potential measurements demonstrate that between seven and nine water molecules are associated with the ion as it permeates through the gramicidin channel (Rosenberg and Finkelstein, 1978; Dani and Levitt, 1981; Levitt, 1984). These data and MD calculations (Mackay et al., 1984; Chiu et al., 1989; Åqvist and Warshel, 1989; Jordan, 1990; Roux and Karplus, 1991) suggest that the channel incorporates 8–10 polar moieties. We chose to model the aqueous pore by nine water molecules, represented by freely rotating point dipoles located in spherical cavities at equally spaced positions along the z axis of the channel.

With an ion present, it was substituted for one of these dipoles. The diameter of the spheres simulating both the water molecules and the ion was initially set equal to 3 Å. Our description of gramicidin was limited to the 32 carbonyls of the peptide backbone that form the lining of the aqueous pore. These were modeled as rigid dipoles of length 1.24 Å with their positive (C) ends fixed and their negative (O) ends mobile. We chose as the initial arrangement of the carbon atoms the model determined by Koeppe and Kimura (1984), inverted to account for the fact that the β-helix is right handed (Arseniev et al., 1985; Nicholson and Cross, 1989). CO bending is described by an harmonic restoring force, $U_{bend} = k_{bend} (\theta - \theta_0)^2/2$. Because the COs are alternately antiparallel, the θ_0 values were chosen equal to 0 or π, essentially the locations of the O atoms in the 0 K, Koeppe-Kimura structure. To avoid oxygen penetration into the "core" of ion and waters, a hard core potential was introduced. The core radius was chosen as 1.5 Å. The force constant k_{bend} was assigned the value, 6×10^{-20} J, comparable to that describing low energy torsional motions in polypeptides (e.g., (Weiner et al., 1984)). All calculations were carried out at 300 K.

Our calculations focused on rotational relaxation, i.e., processes occurring on time scales of picoseconds or longer. Thus electronic relaxation, which contributes to the dielectric properties of matter, was explicitly excluded. Electronic relaxation gave rise to the high frequency permittivity, which contributes to dielectric behavior in all materials and is the dominant term in nonpolar fluids. We accounted for these processes by introducing the background dielectric permittivity $\epsilon_{background}$ chosen to be two (Partenskii and Jordan, 1992b). To simplify the electrostatic calculations, the bulk electrolyte was assigned a dielectric constant $\epsilon = \infty$. Because $\epsilon_{water} \sim 80$, the errors introduced by this approximation were always small, and decreased with increasing ionic strength (Partenskii et al., 1994). The boundary between the low ϵ domain and "bulk solvent" was displaced a distance 1–2 Å relative to the membrane surface. This "Helmholtz layer" (Bockris and Reddy, 1977; Partenskii et al., 1991b) was introduced for two reasons: to account for the finite size of the water molecules and their possible orientational ordering (and thus lower permittivity) at the surface of the membrane; and to avoid unphysical energy anomalies that arise if a point charge (the exterior carbonyl oxygen) is located too close to the boundary of the highly polarizable "bulk" region. The influence of the location of this "image plane" on computational results is discussed below. The model provided a far more realistic description of the peptide than our previous "rings of charge" approach (Partenskii et al., 1994). It also benefited from the advantages of our SMC approach to the description of high frequency polarization modes and of the interaction of the channel's interior with bulk water.

The energetics of permeation were decomposed into a number of distinct thermodynamic steps enumerated previously and described in more detail here. The overall process required exchanging an ion, taken from bulk electrolyte, for a water removed from the channel. This was done in stages, passing through an intermediate vacuum state (with a 1 atm reference state): 1) Transfer of an ion from bulk water to vacuum; the free energy is the negative of the free energy of hydration, $-\Delta G^{ion}_{hydration}$. 2) Transfer of the ion from vacuum

to the uniform dielectric background; the associated free energy change is $\Delta G^{ion}_{vacuum\to\epsilon}$. 3) Transfer of an ion from the uniform dielectric to a site in the channel, exchanging it for the water molecule at that site and returning the water molecule to the uniform dielectric; the free energy change is $\Delta G_{stab} = \Delta G^{ion}_{\epsilon\to channel} + \Delta G^{water}_{channel\to\epsilon}$. 4) Removal of the water from the uniform dielectric to vacuum followed by condensation, a free energy change of $-(\Delta G^{water}_{vacuum\to\epsilon} + \Delta G^{water}_{vaporization})$.

Step 3 contrasts the free energy for transferring an ion from the uniform dielectric to the channel with the corresponding process for a water molecule; we defined this free energy difference as the "stabilization free energy." The total free energy change in transferring an ion to any site in the channel (the permeation free energy) is then

$$\Delta G_{perm} = \Delta G_{transfer} + \Delta G_{stab} \tag{1}$$

where

$$\Delta G_{transfer} = -\Delta G^{ion}_{hydration} + \Delta G^{ion}_{vacuum\to\epsilon} - \Delta G^{water}_{vacuum\to\epsilon} - \Delta G^{water}_{vaporization}. \tag{2}$$

Eq. 2 accounts for free energy changes in removing an ion from water and inserting it into the infinite low ϵ domain and simultaneously removing water from this low ϵ region and adding it to bulk water; this free energy is independent of the ion's position in the channel. We estimated it using experimental data and empirical models. The stabilization component was computed using thermodynamic integration.

The stabilization energy, ΔG_{stab}, is the difference between two terms: the free energy of interaction of an ion at a site in the channel with the pore waters, the channel forming peptide, the lipid membrane, and the surrounding solvent and the corresponding free energy of interaction when a water molecule is at that site. This is the free energy for exchanging an ion, taken from the infinite continuum background with $\epsilon = 2$, with a water dipole in the channel. It was computed by transmuting a channel water dipole into an ion and simultaneously transmuting the ion in the continuum background into a water molecule (because $\epsilon_{background}$ was unaltered in this process, the self energies of both ion and dipole did not change and did not influence ΔG_{stab}). To accomplish this we placed both a charge kq and a dipole $(1 - k)p$ at a particular site, where p is the water dipole moment, 1.86 Debye; the parameter k is continuously variable from 0 to 1. Thus, $k = 0$ corresponds to the ion-free pore, containing nine water molecules, whereas $k = 1$ describes an ion and eight water dipoles in the channel. The total free energy change is given by

$$\Delta G_{stab} = \int_0^1 dk \left\langle \frac{dH}{dk} \right\rangle \tag{3}$$

where

$$\langle(\cdots)\rangle = \frac{1}{Z}\int_{(\Omega)} d\Omega(\cdots)\exp[-\beta H(\Omega, k)] \tag{4}$$

is the canonical statistical average and

$$Z = \int_{(\Omega)} \exp[-\beta H(\Omega, k)]\, d\Omega \tag{5}$$

is the partition function. Consideration of ions of different size, $R \neq R_0 = 3$ Å was easily done by including an additional "cycle" of thermodynamic integration. The final state in the integral of Eq. 3 was Ion($R = R_0$) + 8 Waters. This sometimes was transmuted further to Ion(R) + 8 Waters with $R \neq 3$ Å. The corresponding perturbation to the Hamiltonian was represented as $V(\lambda) = \lambda(H(R) - H(R_0)$. Using Eq. 3 the corresponding free energy change is

$$\Delta G_{stab} = \int_0^1 dk \left\langle \frac{dH}{dk} \right\rangle + \int_0^1 d\lambda \langle [H(R) - H(R_0)] \rangle_{k=1}. \tag{6}$$

In what follows we omitted the argument R (or R_0) whenever $R = R_0$ or the R dependence was not at issue. The Hamiltonian of the system can be represented as follows:

$$H = H_w + H_I + H_{CO} + H_{w,I} + H_{I,CO} + H_{w,CO} + H_{hardcore}. \tag{7}$$

H_w describes the interaction of water dipoles (including the variable one, $(1 - k)p$) with each other and with their images; H_{CO} is the same for the 32 carbonyl subsystem, including the elastic energy; H_I is the ionic interaction with its own images; the next three contributions describe the electrostatic interaction between corresponding subsystems; the final term is a hard core component introduced to keep carbonyl oxygens from penetrating either the ion or the water. Detailed description of the terms contributing to Eq. 7 is provided in the Appendix.

DETAILS OF THE MONTE CARLO APPROACH

To evaluate ΔG_{stab} (Eqs. 3 and 6) we used an MC approach and applied the Metropolis algorithm (MA) (Metropolis et al., 1953), which mimics the statistical integral with the Boltzmann factor $\exp(-\beta H)$ using a special acceptance-rejection procedure. The configuration space of the system corresponded to the various orientations of 32 CO molecules and eight or nine water molecules. This continuous space was then reduced to a discrete set of states. Each node in the corresponding matrix described some set of the orientations of the 41 particles and, therefore, some value of the Hamiltonian H. From numerical experiments we found that to attain an overall accuracy ≤ 2 kJ mol^{-1} it was sufficient to limit consideration to 72 orientations for each particle (6 for the polar angle θ and 12 for the axial angle ϕ). The total number of states was 72^{41}, which is practically infinite, and direct calculation of the statistical integrals is impossible. The MA provided an approach that, in principle, treated this problem.

In practice the analysis of a system with short-range interaction (like an Ising model or a hard sphere gas) was

efficient because the interaction distance was limited. Application of the MA got ever more complicated as the effective interaction radius increased. In our case long-range electrostatic interactions were important, the effective interaction length was ∞, and changing the state of one particle influenced all other particles. A sensible way to handle the associated problems was based on the concept of "precalculation." For each configuration of the system we first calculated as many energy components and other functions as possible, so that at each step of the MA the functions were taken from the storage instead of being calculated de novo, resulting in dramatic economies of time. There were evident limitations to this approach because, the amount of data that could be precalculated was restricted by the size of the RAM. Therefore it was necessary to represent and store information in the most compact way. This was done by exploiting the symmetry of the system and the specific structure of some of the sums appearing in the Hamiltonian.

Another possible computational black hole was the thermalization procedure preceding the statistical calculations in the MC approach. The choice of the number of steps necessary for sufficient thermalization was based on experiment and common sense. Preliminary analysis indicated that the main source of inaccuracy in the free energy calculations was the small k part of the integral Eq. 3 ($k \leq 0.2$). This region required special attention with respect to the number of thermalization cycles, which was varied between 10,000 and 50,000 (Koonin, 1986). We found further that the necessary precautions were dependent on ionic position. In general the conditions were less stringent for an ion near mid-channel. This was reasonable because here the ion was effectively interacting with more particles (it had more near neighbors) than at the edge of the channel. To destroy possible correlations introduced by imperfections in the random number generator we used the technique described by Koonin (1986). Numerical analysis indicated that a δk step of 0.05 for $k > 0.2$ and of 0.025 for $k \leq 0.2$ was sufficient to provide an accuracy of 1–2% in the integrals, Eq. 3 and 6. In the integration varying ionic size, Eq. 6 a λ step of $\delta\lambda = 0.05$ is sufficient.

To check the accuracy of the procedure, to select the appropriate parameters for the calculation of statistical averages (Binder, 1979; Koonin, 1986) and to choose the step sizes for integration over k and λ, we used two different approaches: internal testing and comparison with direct calculation. For the first we performed numerical experiments based on the calculations of the channel properties (energy, free energy, average dipole moments, average orientation of carbonyl groups) using different choices of the parameters. The aim was to find the values of the parameters that provided reasonable accuracy at minimal computational expense (both CPU time and RAM). For the second, we compared the MC results of restricted models with the results of direct statistical calculations for the same models, described elsewhere (Partenskii and Jordan, 1992a; Partenskii et al., 1994). For the parameters chosen we obtained reliable results (accuracy in free energy ≤2 kJ mol^{-1}) in ~2 h for each ionic position using an IBM-350, RS-6000 with 64 MB RAM.

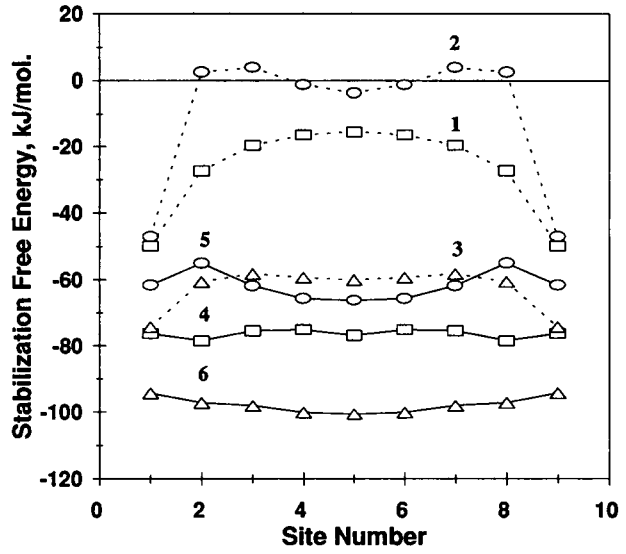

FIGURE 2 Effect of carbonyl groups and water on the cation stabilization free energy profile. An image plane separation of 31 Å is used; the carbonyl partial charge, q_C is $0.5e_O$. The ionic radius is 1.5 Å. Two sets of three free energy calculations are presented, the first set with no pore water present (*dashed lines*), the latter three with the eight pore waters included (*solid lines*). The symbols □, ○, and △ indicate computations with no COs present, with the COs frozen in their native alignment, and with the COs reorienting in response to interaction with the ion (and water), respectively. The six cases are: 1) free energy decrease due to image interaction with electrolyte; 2) influence of native gramicidin charge distribution; 3) influence of reorienting gramicidin carbonyls; 4–6 are the same as 1–3, only now with eight pore waters included. The same ionic radius is used in Figs. 2–6.

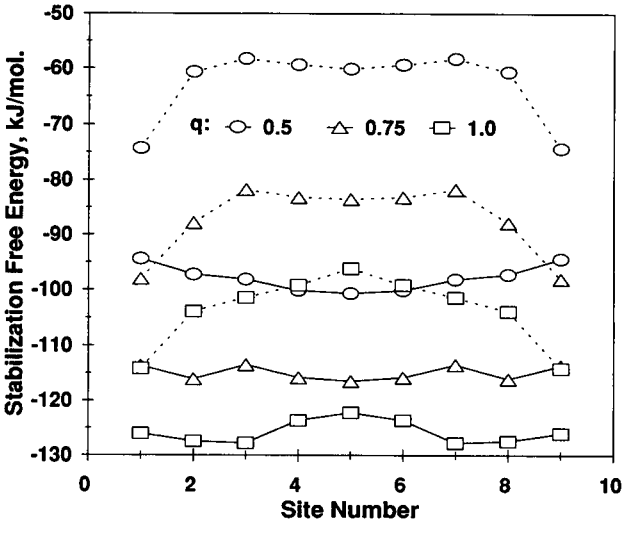

FIGURE 3 Influence of varying q_C on the cation stabilization free energy profile. An image plane separation of 31 Å is used; the carbonyl partial charges, q_C, are $0.5e_O$ (○), $0.75e_O$ (△), and $1.0e_O$ (□). Increasing q_C increases cation stability in the channel. In all cases carbonyls reorient in response to the ion. Two sets of computations are contrasted: without (*dashed lines*) and with (*solid lines*) pore water present.

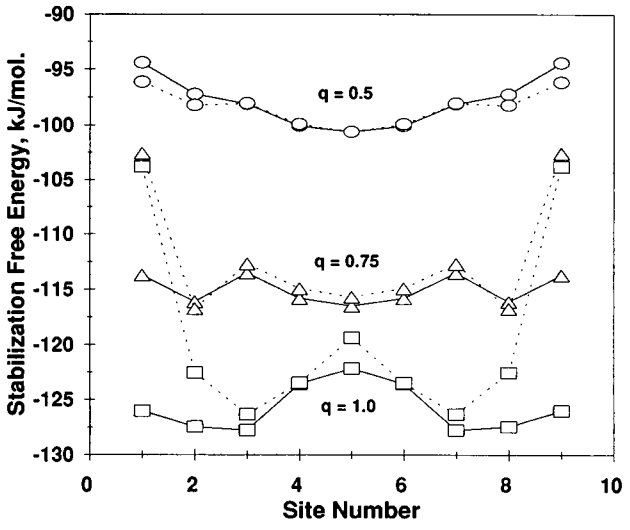

FIGURE 4 Influence of image plane separation and q_C on the cation stabilization free energy profile. Two image plane separations, 31 Å (*solid lines*) and 29 Å (*dashed lines*), are contrasted; the carbonyl partial charge, q_C, varies from $0.5e_O$ to $1.0e_O$ (symbols are the same as in Fig. 3). In all cases pore water is present, and the carbonyls reorient in response to the permeant ion.

RESULTS AND DISCUSSION

Ionic stabilization in the channel; internal barrier

Figs. 2–5 illustrate the influence that different components of the interaction Hamiltonian (Eq. 7) and the parameters q_C and L have on a cation's (and in some cases on an anion's) stabilization free energy, ΔG_{stab}. ΔG_{stab} is always negative and compensates (totally or partially) for the transfer free energy (Eq. 2) required in taking an ion from bulk water and exchanging it for a water dipole removed from the uniform, infinite, $\epsilon = 2$, dielectric. This section focuses on ΔG_{stab},

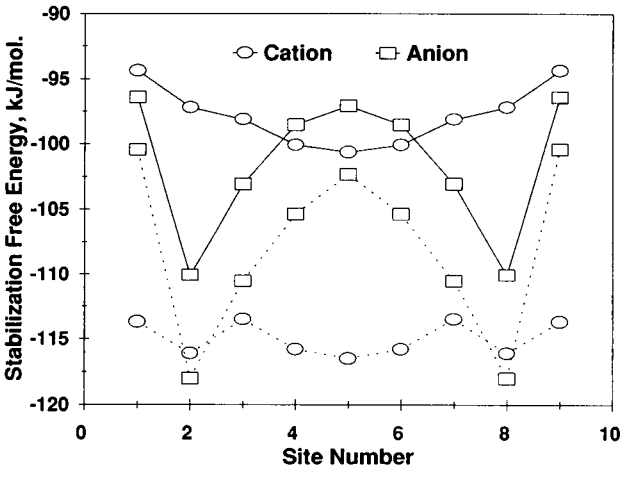

FIGURE 5 Comparison of cation (○) and anion (□) stabilization free energy profiles for an ion in a pore with eight waters, surrounded by reorienting carbonyls. An image plane separation of 31 Å is used; two carbonyl partial charges, with q_C values of $0.5e_O$ (*solid lines*) and $0.75e_O$ (*dashed lines*), are contrasted.

which completely determines the shape of the translocation free energy profile. The position independent contribution of $\Delta G_{transfer}$ is discussed later.

Fig. 2 illustrates the independent and coupled influence of both channel water and the carbonyls on cation stabilization at nine equally spaced sites in the gramicidin-like channel. Here, the Helmholtz layer is 2 Å wide (L = 31 Å) and the partial charge assigned to the CO groups, q_C, is the AMBER value, $0.5e_O$ (Weiner et al., 1984); the carbonyl groups thus contribute ~3 Debye to the peptide dipole moment, slightly less than its full value, typically 3.5 Debye (Hol, 1985). Values as large as 6 Debye have been suggested (Wada, 1976), i.e., a q_C of $\sim 1.0e_O$, but this certainly overcompensates for any influence of backbone amines and α-carbons. Two sets of calculations are illustrated, with and without channel water present. In each instance we considered three cases: no carbonyls, carbonyls frozen in their native orientation, and carbonyls re-equilibrating in response to the ion. Consider first the set without channel water. The ion only curve (1) is simply the stabilization energy due to finite slab thickness, i.e. ion interaction with its own images in the bulk electrolyte (Parsegian, 1969; Partenskii and Jordan, 1992b). Interaction with the fixed carbonyls (2) is destabilizing because the gramicidin helix has a permanent quadrupole moment, positive at the dimer junction and negative at the channel mouths (Sung and Jordan, 1987a). The dimer's native charge distribution generates an effective surface dipole potential at each mouth creating an electrical barrier reducing cation stability in the pore. Because the carbonyls are antiparallel, this contribution to the electrical potential is roughly constant inside the channel, which accounts for the major free energy differences between curves 1 and 2 taking place between sites 1 and 2 (or 9 and 8). Stabilization by the peptide arises because the carbonyl oxygens reorient (3) and are displaced toward the ion. This reorientational stabilization is greatest near the channel midpoint, where the long-range modulating influence of the electrolyte is weakest. With the water chain present there is additional stabilization; without carbonyls (4) this is because of the combined effect of waters and images. Again, the native peptide charge distribution is destabilizing (5) and the major change from curve 4 takes place between sites 1 and 2. Overall, the greatest stabilization arises with coupled ion-water-carbonyl reorientation (6). This last free energy profile is particularly interesting because it is essentially flat, corresponding to a negligible translocation free energy barrier. As neighboring sites are separated by 3 Å it is conceivable that important molecular details have been overlooked. To check whether this coarse grid could be problematic, we shifted the whole chain ±0.5 Å at each ion site; in no case did the corresponding free energy change exceed ±(2–3) kJ mol^{-1}. Consequently there is very little variation in the permeation free energy associated with cation translocation through the channel, in fundamental agreement with the Brownian dynamics analysis of conductance data (Jakobsson and Chiu, 1987). It should be stressed that the SMC model, as we have imple-

mented it to date, is not designed to determine a fine grained stabilization potential. By localizing both the ion and the water dipoles, and considering only the influence of the peptide carbonyls, we only describe grosser aspects of stabilization. Any fine structure associated with specific binding sites is likely to be lost.

Fig. 3 illustrates the influence of varying q_C from $0.5e_O$ to e_O, demonstrating that the translocation profile is fairly flat regardless of the choice of q_C. In these calculations the Helmholtz layer is again 2 Å wide (L = 31 Å). We present data for carbonyls re-equilibrating in response to the ion, with and without water present. As q_C increases, there is additional stabilization that is not linearly dependent on q_C. At the channel midpoint there is a 25 kJ mol^{-1} drop in free energy when q_C increases from $0.5e_O$ to $0.75e_O$; the energy only drops another 10 kJ mol^{-1} as q_C increases further to e_O. Interaction with the water chain leads to added stabilization, largest (40 kJ mol^{-1}) at small q_C and only ~25 kJ mol^{-1} at the largest q_C. In all cases translocation is essentially barrier free.

Fig. 4 illustrates the effect that varying the image plane separation has on ΔG_{stab} in a water filled channel, again accounting for carbonyl re-equilibration. In the channel interior results are insensitive to L. However, this is not so near the mouth of the channel, reflecting the fact that all sources have been described as point charges. To circumvent the anomalies, the charge distribution of the ion and carbonyls near the mouth must be modeled more accurately; close to a dielectric discontinuity, electrical sources cannot be described as point charges (Kharkats and Ulstrup, 1991; Beglov and Roux, 1994). In the internal part of the channel (further than 3–5 Å from the entrance) the results are not sensitive to conditions at the interface. It is only near the channel mouth that image plane positioning has an effect, which is more pronounced as q_C increases. The results for the smallest q_C, $0.5e_O$, are clearly not image plane sensitive, suggesting that the L = 31 Å results for the larger values of q_C are probably not influenced by image plane singularities.

Fig. 5 contrasts ΔG_{stab} for anions and cations (both 3 Å in diameter) as functions of q_C (with L = 31 Å). As just discussed, the free energy barrier for cationic translocation is small; even at "fine resolution" (permitting ± 0.5 Å displacements relative to the positions illustrated) it does not exceed 6 kJ mol^{-1}. The anionic profiles are strikingly different. Regardless of q_C there is a significant translocational barrier, ~15 kJ mol^{-1}. Of even greater interest is the total stabilization free energy (the difference between the global minima). For the smaller value of q_C, gramicidin's interaction with the anion is more favorable than its interaction with the cation, by ~10 kJ mol^{-1}. As q_C increases to 0.75, equivalent to a peptide dipole of 4.5 Debye, this difference drops, but it is still ~2 kJ mol^{-1}. These results are similar to those of a molecular mechanics comparison of the interaction of Cl^- or Cs^+ and a few (0–4) water molecules with the gramicidin backbone (Sung and Jordan, 1987b). The earlier calculation (which considered both carbonyl and amine groups) also showed that the peptide interacts more favorably with the anion than with the cation. Both old and new results are at odds with the original rationalization of valence selectivity in gramicidin, which suggested that cation interaction with the channel was favored over its interaction with an anion (Urry et al., 1981).

To understand why the anion interacts more effectively with gramicidin, consider the native quadrupolar charge distribution (fixed COs); as already indicated, it generates an effective surface dipole potential at each mouth. This destabilizes cation occupancy and favors anion occupancy. Within the channel this cation-anion difference is largest at site 2 (42 kJ mol^{-1}) and drops steadily to 21 kJ mol^{-1} at the midpoint; the difference between the global minima is ~35 kJ mol^{-1}. Carbonyl reorientation stabilizes both cation and anion; however, attraction of the oxygens by a cation necessarily has greater energetic consequences than the repulsion by an anion; thus both site specific and global cation-anion differences are reduced, but not eliminated. The peptide quadrupole interacts more effectively with an anion than a cation; carbonyl reorientation provides only partial compensation. The barrier to anion translocation also reflects gramicidin's generation of an effective surface dipole. This creates the anionic well near site 2 (in contrast to the cationic peak); again carbonyl reorientation has a much greater influence on the cation profile. Whereas internal structure in the cation profile is damped out, the anionic translocation barrier drops only slightly, from ~15 to ~13 kJ mol^{-1}. These polarity dependent differences will be altered if the amine groups are specifically taken into consideration. However, given the results of the earlier molecular mechanics study (Sung and Jordan, 1987b), we would still expect ΔG_{stab} to be greater for anions.

Table 1 decomposes the stabilization free energy difference between the two states, 9 waters in the channel and an Ion + 8 waters in the channel, into enthalpic and entropic contributions. Generally the entropic term does not exceed ~10% of the total free energy. Thus, stabilization energies and the shape of the internal barrier can usually be estimated by the (much simpler) calculation of ⟨H⟩.

An important result of our calculations, consistent with molecular dynamics studies (Mackay et al., 1984; Jordan, 1990; Roux and Karplus, 1991), is that there are only local perturbations of the polar groups by the translocating ion. There is noticeable tilting of the COs from their equilibrium orientations only for groups for which the oxygen atoms are closest to the ion. Depending upon whether the ion is near

TABLE 1 Stabilization free energy, enthalpy and entropy at different sites

	$q_C = 0.5e_o$			$q_C = 0.75e_o$		
Position	−⟨H⟩	−G	-TΔS	−⟨H⟩	−G	-TΔS
1	41.3	38.1	3.2	50.2	45.8	4.4
2	41.2	39.2	2.0	48.2	46.8	1.4
3	42.1	39.6	2.6	48.0	45.8	3.2
4	46.2	40.4	5.8	49.5	46.7	2.8
5	44.0	40.6	3.4	51.6	47.0	4.6

Cation radius is 1.5 Å.

the mouth or in the channel interior, there are only 3 or 4 such oxygens. Preliminary analysis (for $q_C = 0.5e_O$ with the ion in the middle of the channel) shows that holding most carbonyls fixed (in practice, about 25 of them) in the course of MC trial moves permits reproduction of the exact free energy to within 3–5 kJ mol^{-1}. This observation can probably be used to further optimize the computational algorithm thus permitting us to explicitly consider the influence of the backbone amines and α-carbons and the polar side chains.

Transfer contribution and the permeation profile; the basis for cation selectivity

So far we have considered the influence that pore water, the peptide and the membrane have on ionic stabilization in the channel. The translocation free energy profile was determined by the stabilization free energy. The global minima in ΔG_{stab} were comparable for a similarly sized cation and anion, with the anionic well somewhat deeper. The shapes of the profiles were very different, essentially flat for cations and with a marked internal barrier for anions. In the overall permeation process (Eq. 1) these (negative) contributions compensate for the free energy required to transfer an ion from the high ϵ medium (bulk water) to the low ϵ background medium with $\epsilon = 2$ and simultaneously exchange it for a water dipole. We now analyze the transfer component (Eq. 2), which is decomposed into separate contributions from both ions and water.

The ion contributes the terms $(\Delta G^{ion}_{vacuum\to\epsilon} - \Delta G^{ion}_{hydration})$ to the transfer free energy. The hydration part, the free energy for transferring an ion from water to vacuum, has been extensively studied both theoretically and experimentally. There is an enormous literature on this topic because its absolute determination is not possible (see e.g., Noyes, 1964; Friedman and Krishnan, 1973; Marcus, 1994). Theoretical models have evolved from Born's original idea (Born, 1920), which envisaged the process in continuum terms,

$$\Delta G^{Born}_{hydration} = -\frac{q^2}{2R_I}\left(1 - \frac{1}{\epsilon_{water}}\right), \qquad (8)$$

where q is the ionic charge, R_I the crystal radius and ϵ_{water} the dielectric constant of bulk water. However, ionic hydration involves structural reorganization of water in ways not accounted for by a continuum model. Subsequent work has been of two general types: attempts to compute $\Delta G^{hydration}_{ion}$ directly using MD, with its focus on short range interactions (Hirata et al., 1988; Straatsma and Berendsen, 1988; Roux et al., 1990; Beglov and Roux, 1994), or Warshel's reaction field approaches, all designed to ensure that long range electrostatics is properly treated (Warshel, 1979; Warshel and Russell, 1984; Lee and Warshel, 1992); modification of Eq. 8 by introducing either an effective ionic radius (Latimer et al., 1939; Rashin and Honig, 1985; Jayaram et al., 1989) or an effective local ϵ (Noyes, 1962; Noyes, 1964; Liszi and Ruff, 1985) or both (Marcus, 1994). Rather than extending our model to describe ionic solvation in water, we estimated $\Delta G^{hydration}_{ion}$ from experimental data. Unambiguous determination of an energy zero (the absolute enthalpy change in the process $H^+_{aq} \to H^+_{vacuum}$) is not possible; the proposed values vary between 1091 and 1103 kJ mol^{-1} with quoted uncertainties in each determination of $\pm$5–10 kJ mol^{-1} (Marcus, 1987). Consequently different analyses yield different values for $\Delta G^{ion}_{hydration}$. Rather than adopting a particular data set, we averaged the values suggested. There is consequently an uncertainty of $\pm$10 kJ mol^{-1} in our numbers. To compute $\Delta G^{ion}_{vacuum\to\epsilon}$, we employed the continuum approximation

$$\Delta G^{ion}_{vacuum\to\epsilon} = \frac{q^2}{2R_I}\left(\frac{1}{2} - 1\right) = -\frac{q^2}{4R_I}, \qquad (9)$$

choosing the crystal radius for the size of the cavity. Because our model accounts explicitly for the reorientation of the carbonyl oxygens and the water dipoles that lead to differences between the size of the effective cavity in water and the channel, a point stressed by Roux and Karplus (1993), such contributions are automatically included in ΔG_{stab} in much the same way as they are in Warshel's reaction field treatments of ionic solvation (Warshel, 1979; Warshel and Russell, 1984; Lee and Warshel, 1992). Hydration free energies and ionic radii are listed in Table 2 for three cations (Cs^+, Rb^+ and K^+) and three anions (Cl^-, "1.5"$^-$ and F^-); "1.5"$^-$ indicates an hypothetical anion of 1.5 Å radius. Whereas the free energies have an intrinsic uncertainty because of the ambiguity in establishing the free energy zero, a shift in the reference value affects all univalent cationic terms equally. Univalent anionic free energies would be shifted the same amount, but in the opposite direction.

Water contributes $-(\Delta G^{water}_{vacuum\to\epsilon} + \Delta G^{water}_{vaporization})$ to $\Delta G_{transfer}$. The first term can be computed and the latter is just the free energy of vaporization, +8.7 kJ mol^{-1} at 25°C (all reference states are 1 atm in the vapor and 1 M electrolyte in solution). We have previously analyzed the transfer of a dipolar cavity from the vacuum to the uniform background (Partenskii et al., 1994); for a water dipole in a 3 Å cavity we found the free energy to be −7.7 kJ mol^{-1}, which is in reasonable agreement with the value that can be

TABLE 2 Ionic radii and free energies of hydration*, transfer‡, permeation§ and stabilization‡,¶ for selected ions

Ion	Radius (Å)	$\Delta G^{ion}_{hydration}$ (kJ mol^{-1})	$\Delta G_{transfer}$ (kJ mol^{-1})	ΔG_{perm} (kJ mol^{-1})	ΔG_{stab} (kJ mol^{-1})
K^+	1.33	−329.8	67.8	−25.2	−93.0
Rb^+	1.48	−310.2	77.8	−11.0	−88.8
Cs^+	1.70	−282.0	76.8	−7.9	−84.7
F^-	1.33	−445.4	183.4	77.8	−127.9
"1.5"$^-$	1.50	−405.4	173.0	71.5	−119.7
Cl^-	1.81	−326.2	133.4	38.6	−107.9

*Free energies are averaged values from various sources (Noyes, 1962; Noyes, 1964; Marcus, 1983; Marcus, 1991; Parsons, 1959; Burgess, 1978; Friedman and Krishnan, 1973). Ionic radii are also slightly source dependent; the associated uncertainties in ΔG_{perm} never exceed 2 kJ mol^{-1}.

‡See text.

§For cations the values are maximum well depths; for anions they are entrance barriers.

¶Stabilization energies are measured relative to the maximum well depth for all ions.

extracted from computer simulations of aqueous solvation (Beglov and Roux, 1994). The total transfer energy (in kJ mol^{-1}), also given in Table 2, is thus

$$\Delta G_{\text{transfer}} = -1 - \Delta G^{\text{ion}}_{\text{hydration}} - \frac{q^2}{4R_I}. \qquad (10)$$

As is evident from Table 2, there are significant differences between the hydration (and thus the transfer) free energies for anions and cations of the same size. These differences are well known (Noyes, 1964; Friedman and Krishnan, 1973; Marcus, 1994), but their biophysical implications are not always appreciated (Collins, 1995). They have their origin in the asymmetry of water's molecular charge distribution (its quadrupole moment). Because our approach to computing the stabilization free energy, with a point dipole in the center of a spherical cavity, did not account for this asymmetry, a correction must be applied before discussing permeation. This can be done simply by shifting the point dipole to the center of mass of the charge distribution, ~0.3 Å off center. Estimates based on this model, assuming a hexacoordinate hydrated ion surrounded by a uniform dielectric medium in which $\epsilon_{\text{water}} \sim 80$, yielded ~60 and ~70 kJ mol^{-1} differences between the hydration energy of anions and cations with R_I = 1.5 and 1.33 Å, respectively. These accounted for somewhat over half of the anion-cation differences presented in Table 2. We have used this model, a displaced dipole, to provide rough estimates of the corrections to the stabilization energy arising from the water quadrupole. The results for ions with R_I = 1.5 Å are presented in Fig. 6 for q_C = 0.5. The correction decreased the absolute value of the stabilizing contribution for the cation by ~5–10 kJ mol^{-1} and increased it by approximately the same amount for the anion. In addition, it slightly changed the shape of the energy profile; there are now two internal maxima (~3 kJ mol^{-1}) in the cation free energy profile. Calculations based on a finer grid, including the other backbone moieties, would generate more structured stabilization free energy profiles.

Following this prescription, we computed permeation free energy profiles for the six ions chosen; we did not consider Li^+ or Na^+ because our model, a linear ion-dipole chain is clearly a poor approximation in this instance. Here the ions moved well off the channel axis during permeation (Skerra and Brickmann, 1987; Sung and Jordan, 1987b; Roux and Karplus, 1993; Elber et al., 1995), which significantly affects the stabilization free energy. In all cases we chose a $q_C = 0.5e_O$, the AMBER value (Weiner et al., 1984), in computing stabilization free energies. This is equivalent to a peptide dipole of ~3 Debye. The permeation free energy profiles are naturally sensitive to this choice because q_C determines the strength of both ion-peptide and water-peptide interaction. Simply increasing q_C to account for the full peptide dipole would lead to an additional ~5 kJ mol^{-1} stabilization of the cation profiles. However, the physical basis for the larger peptide dipole is the influence of the amines and the α-carbons, both neglected in our model. Although less important than the carbonyl groups (their axial dipolar contributions are ~15% that because of the COs), they will affect ΔG_{stab} in a complex manner, unlikely to be reliably modeled by a simple increase of q_C. Unlike the CO dipole, which is essentially axially oriented

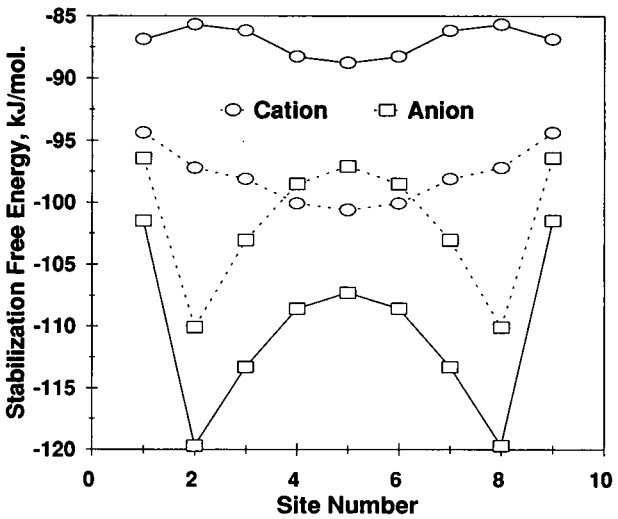

FIGURE 6 Effect of water's asymmetry (the water quadrupole) on the stabilization free energy of anions (□) and cations (○) of 3 Å diameter. A q_C of $0.5e_O$ is used with an image plane separation of 31 Å. Results contrast behavior with (*solid lines*) and without (*dashed lines*) the displaced dipole correction. Displacing the dipole leads to destabilization of the cation and further stabilization of the anion.

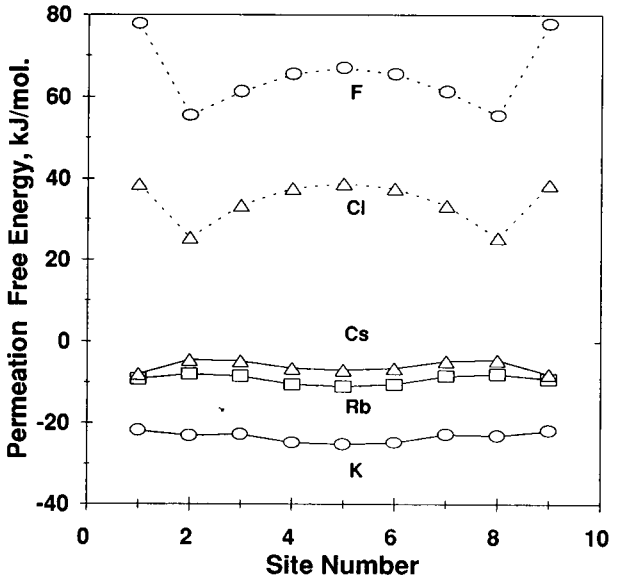

FIGURE 7 Permeation free energy profiles for five selected ions. The channels contain an ion and eight water molecules, surrounded by reorienting carbonyls. A displaced dipole correction is included. An image plane separation of 31 Å is used with a carbonyl charge, q_C, of $0.5e_O$. The reference state in each case is 1 M bulk electrolyte. Ionic radii are listed in Table 2. Ions of about the same size are designated by the same symbols: Cs^+ and Cl^- (△), Rb^+ (□), and K^+ and F^- (○). The solid and dashed lines denote cationic and anionic permeation profiles, respectively.

in native gramicidin, these neglected terms contribute both axial and radial components that can alter the structure of the free energy profiles, not just shift them uniformly. Thus we choose a q_C of $0.5e_O$ rather than assume that the influence of the amines and α-carbons can be described in terms of an adjusted peptide dipole.

Our results are presented in Fig. 7 and Table 2. First consider the cationic permeation profiles: 1) They exhibit binding wells relative to bulk electrolyte. 2) The global translocational free energy barriers are small. 3) The well is smallest for Cs^+ and largest for K^+. 4) Well depths range from 8–25 kJ mol^{-1}. At all sites in the channel the cation is stable with respect to water.

These results are in excellent accord with the gross behavior of potential profiles deduced from experiment (Andersen, 1983; Urban et al., 1980; Eisenman and Sandblom, 1984; Jakobsson and Chiu, 1987). Because of the uncertainty in the absolute hydration free energies, the profiles could be translated ± 10 kJ mol^{-1}; however, each would be affected in the same way. Their relative ordering is not influenced by this uncertainty. Whereas extending the approach to include remaining backbone moieties will modify the energetics of stabilization, it will not significantly alter observations 1 to 3; the actual well depths will be affected and binding sites might appear, but the shifts will be smaller than the $\pm$ 10 kJ mol^{-1} hydration free energy uncertainty. Because our computational method focused on a linear ion-water chain, an approximation only reasonable for the larger monovalent cations (Skerra and Brickmann, 1987; Sung and Jordan, 1987b; Roux and Karplus, 1993), detailed comparison with potential of mean force calculations on Na^+ (Roux and Karplus, 1993; Åqvist and Warshel, 1989) was not possible. However, the internal free energy barriers to K^+ translocation in a periodic poly (L,D)-alanine model for gramicidin are 4 kJ mol^{-1} (Roux and Karplus, 1991), a value close to ours, 3 kJ mol^{-1}.

The anion profiles are strikingly different: 1) There are barriers to ion entry. 2) There are significant free energy barriers to internal translocation. 3) Both entry and internal barriers are larger for the smaller ion. 4) The entrance barriers are large, 39 and 78 kJ mol^{-1} for Cl^- and F^-, respectively. At all sites in the channel the anion is unstable with respect to water (effective binding affinities are between 3×10^4 M and 4×10^9 M).

Even though anions interact more favorably with the channel than do cations (see Figs. 5 and 6), anion entry is effectively forbidden. The fundamental reason for this tremendous polarity dependent difference is that, for ions of the same size, anions bind water much more strongly than cations. Here too, we expect that extension of the model to include the remaining backbone moieties will modify the energetics of stabilization without significantly influencing the major observations.

The data presented in Table 2 serve further to clarify the origin of the anion-cation differences. Our energetic decomposition contrasts effects from transfer of the ion from water to lipid (solvation by water) with those from interaction with the gramicidin pore (solvation by the channel former). Anion-cation differences in the transfer component, $\Delta G_{transfer}$, are $\sim$3 times as large as the corresponding differences in the stabilization term, ΔG_{stab}. Interaction with water is a more important determinant of polarity dependent differences than is interaction with the channel former.

It should be stressed that valence selectivity arises for precisely the same reason first proposed by Eisenman (1962) in his approach to cation selectivity. Permeation represents a competition between binding to water and to a site in the channel, a point noted in theoretical studies of Na^+ interaction with gramicidin A (Åqvist and Warshel, 1989; Roux and Karplus, 1993). Ions that are too strongly hydrated cannot permeate. Usually this consideration is used to interpret selectivity sequences for ions of the same polarity. However, it applies equally well to ions of different polarity. Typically channel sites are themselves charged, and valence discrimination reflects the influence of such side chains. In gramicidin there are no charged side chains, and aqueous hydration becomes a dominant consideration. An analogous observation with respect to differential solvation was made by Andersen and Koeppe (1992) in a discussion of anion-cation differences in transfer free energies from water to formamide and dimethylformamide. Cations are more stable in either formamide than in water; the opposite is true for anions.

We now consider a long standing puzzle in gramicidin biophysics. When crystallized from methanolic solutions containing CsCl, the channel incorporates five ions, three anions and two cations (as well as some methanol of solvation) (Wallace and Ravikumar, 1988; Wallace, 1990); the third cation, required for electroneutrality, is interstitial. Even though in the crystal gramicidin forms a double stranded helix (DS), rather than the head-to-head (HH) dimer more typical of the membrane bound dimer, our stabilization free energy calculations can shed light on this observation. The basic electrical potential of the DS conformer is the same as that of the HH conformer; there is an effective surface dipole at each mouth destabilizing cation occupancy (Sung and Jordan, 1988). The crystal structure demonstrates that here too the carbonyl groups are aligned alternately antiparallel to the channel axis (Wallace and Ravikumar, 1988). The gross pore dimensions of the HH and DS forms are similar (Wallace and Ravikumar, 1988; Smart et al., 1993). Thus we expect that ionic interaction with both HH and DS forms are comparable. Certainly the electrical properties of membrane bound DS channels provide evidence for this (Durkin et al., 1992); they are cation selective and they exhibit single channel conductances only slightly smaller than HH channels. Thus, the stabilization free energies for ions interacting with a water-filled DS conformer should not be much different. If changing solvent also has little influence on anion-cation differences (consistent with transfer energetics to non-aqueous solvents (Marcus, 1983)), we would expect no substantial change in polarity dependent differences in ΔG_{stab} for ions interacting with a water-filled HH channel or a methanol filled DS

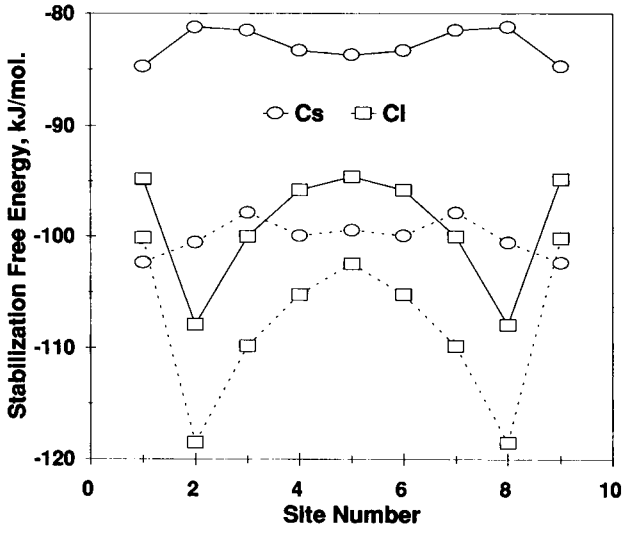

FIGURE 8 Comparison of Cs^+ (○) and Cl^- (□) stabilization free energy profiles for an ion in a pore with eight waters surrounded by reorienting carbonyls. A displaced dipole correction is included. An image plane separation of 31 Å is used; two carbonyl partial charges, with q_C of $0.5e_O$ (*solid lines*) and $0.75e_O$ (*dashed lines*), are contrasted. The ionic radii are those of Table 2.

channel. As seen in Figure 8, with $q_C = 0.5e_O$ or $0.75e_O$, the stabilization free energy for Cl^- is greater than that for Cs^+, and there is a well articulated low energy site near the channel entrance. Permeation is a competition between association with the solvent and association with the channel; cation and anion can interact individually with the channel. Crystallization requires electroneutrality. If the channel preferentially incorporates one ion rather than the other, the favored ion is that which is more stable in the channel. Because chloride's stabilization free energy is greater, anion occupancy is preferred. The experimental results demonstrate that the channel is stabilized by included ions. Thus, if an ion is to be included, Cl^- is favored over Cs^+. It should be noted that this observation may not apply to all anions. In gramicidin crystallized from methanolic CsSCN, the cation binding sites are further apart (Wallace, 1990) and it is unlikely that the channel binds three anions; however, the linear SCN^- interacts with the solvent in a much different fashion from the spherical Cl^- and a quite different stabilization free energy profile can be expected.

Another instance where differences between anion and cation hydration energies appear to affect permeation energetics is in the recently designed "nanotubes" (Ghadiri et al., 1994). These are larger bore channels than gramicidin, ~8 Å diameter. However, their internal structure exhibits similarities; the tubes are formed by peptide rings held together by hydrogen bonds between carbonyl and amine groups on different rings; the COs are also alternately antiparallel. The nanotube is clearly cation selective, favoring Cs^+ permeation over Cl^- by about a factor of six (Buehler et al., 1995). Given the large size of the channel, its electrical banality, and the fact that Cs^+ and Cl^- have equivalent aqueous conductivities (Jordan, 1979), one obvious rationalization for selectivity is the hydration energy of the ions. If partial dehydration is required during permeation, this could account for the channel's selectivity; cesium is dehydrated more easily and it would thus be favored over chloride.

Recent work has demonstrated that the uncharged peptide Ac-$(LSSLLSL)_3$-$CONH_2$ is cation selective (Kienker and Lear, 1995). Whereas the channel conducts both K^+ and Cl^-, there is a distinct preference for K^+. The pore is mid-sized (diameter ~8 Å) and presumably formed by aggregation of parallel α-helices (Kienker and Lear, 1995). The helix dipole potential would affect the free energy profiles of both ions equivalently (with binding on opposite sides of the channel). However, here too, if partial dehydration occurs during permeation, this would contribute to charge selectivity. If there is an entry barrier, it is smaller for cations. It must be stressed that the permeation mechanism is clearly more complex; valence dependent dehydration asymmetry does not readily account for the observation that the permeability ratio changes substantially depending on whether dilution occurs on the side of the membrane held at a positive or negative potential (Kienker and Lear, 1995).

On an even more speculative note, differential dehydration may contribute to well known physiological differences between anion and cation channels (Hille, 1992). In general anion channels are less selective than cation channels. They also appear to be of a generally larger cross section. Both these phenomena may be significantly influenced by the effect of polarity on ionic dehydration. Highly discriminating selectivity filters tend to require a narrow constriction, and with it substantial dehydration, that is energetically far less costly for cations than for anions of the same size. That anion channels tend to have larger cross sections could well be complementary; dehydration is unfavorable and the permeating moiety should be larger. A similar point with respect to dehydration energetics has been made by Andersen and Koeppe (1992) in discussing polarity dependent differences in transfer free energies of ions from water to non-aqueous solvents. It should be noted that other explanations are possible. Unlike the alkali cation-water dimer complexes, the halide-$(H_2O)_2$ complexes are non-linear with favorable water-water interactions (Sung and Jordan, 1986; Cieplak et al., 1987); these polarity dependent coordination differences could have structural implications for physiological channels.

The MC extension of the SMC approach is a powerful tool for understanding important features of ion-water-channel interaction in gramicidin. Future work will incorporate gramicidin's amines and α-carbons. Because free energy computations can be rapidly completed, the method is ideally suited to perturbative studies; we will apply it to analysis of the influence of mutating gramicidin's amino acid side chains (Russell et al., 1986; Mazet et al., 1984; Becker et al., 1991). A major limitation is treating the channel contents as a linear chain; modifications permitting off axis ion motion so that the approach can be extended to Na^+ and Li^+ permeation are planned. Another limitation is the artificial distinction between discrete channel water and continuum electro-

lyte, and thus fixing the number of particles in the channel. This can be dealt with by recasting the problem using a grand canonical formalism; it will then be possible to apply the SMC method in the intermediate region between bulk and the channel interior. Thus extended, it will be possible to study ion-water-channel interaction in physiologically important systems containing wider selectivity regions, and no clear boundaries between the vestibule and the channel; of special interest are nicotinic receptor channels, both anion and cation selective.

SUMMARY

SMC modeling demonstrates that, for ions of the same size, monovalent cations and anions are comparably well stabilized by interaction with gramicidin's aqueous pore; if anything, the anion interacts more slightly favorably with the channel. Whereas anions exhibit significant translocational free energy barriers, cations do not. There are no broad barriers to cation translocation across the channel. Computed permeation free energy profiles for the cations Cs^+, Rb^+ and K^+ display binding wells of 8–25 kJ mol^{-1} relative to the hydrated cations. The permeation free energy profiles for F^- and Cl^- have pronounced energy barriers to ion entry; at all sites in the channel binding affinities are greater than 4×10^9 and 3×10^4 M respectively. The origin of the gramicidin's valence selectivity is the large difference between hydration energies of anions and cations of the same size. Anions bind their waters of hydration much more strongly; channel interaction with anions, although slightly more stabilizing than interaction with cations, cannot compensate for the large hydration energy differences.

APPENDIX

Derivation of the Hamiltonian

In our calculation of the electrostatic energy of the system, we use the method of images and express the long-range interactions in closed forms. Each charge q creates two infinite chains of images: "even" and "odd." Both chains are parallel to the z-axis of the channel and have periods 2L (L is the width of the membrane). The even chain is centered at the real (source) charge, so that the z-coordinates of the images are $z^s_{even}(I) = 2sL + z(I)$ where $s = 0$ corresponds to the real charge and $z(I)$ is its z-coordinate; the odd set is centered at $-z(I)$, so that $z^s_{odd} = 2sL - z(I)$. The image charges are: $q_{even} = q$ and $q_{odd} = -q$. For the point dipoles the coordinates of the images obey the same equations (with $z^0(I)$ now being the dipolar coordinate). The image dipoles in the even chain have the same orientations as the source dipole: $p_{even} = p$. In the odd chain the same is true only for the z-projections ($p^z_{odd} = p_z$), whereas the projections in the xy-plane have the opposite sign ($p^{x,y}_{odd} = -p^{x,y}$).

With these rules it is easy to represent the electrostatic contributions to the system's Hamiltonian as a sum over all images. The sums converge rapidly. For instance, the odd and even image chains for a point charge taken together represent the periodic 1-D lattice consisting of the neutral cells separated by the distances $2L$. Each cell includes two charges, $+q$ and $-q$, separated by the distance $d_{cell} = 2z(I)$. Thus, for distant contributions the field of the cell decays as $\sim r^{-3}$ (a dipolar field). The closer the charge is to the boundary, the smaller is d_{cell} and the more rapid the sums converge. In all cases it is sufficient to only consider the first 10–15 images.

To illustrate the method we explicitly display the terms in $h(k, \Omega)$ which depend on the parameter k and constitute the main distinction between $H(k, \Omega)$ $(\cdots)$ and the Hamiltonians of the simpler systems studied in (Partenskii et al., 1991a; Partenskii et al., 1991b).

$$h(k, \Omega) = h_{I,D} + h_{I,CO} + h_{d',D} + h_{d',CO} + h_{I,d'} + h_{d',d'} \quad \text{(A1)}$$

Here I corresponds to the "ionic" charge k, D to the system of eight dipoles, CO to the system of 32 carbonyls and d^1- to the artificial dipole $(1 - k)p$. Using standard expressions for the electrostatic fields and the summation over the images we find:

$$h_{I,D} = -a_{Id} \sum_{i=1}^{9} \sum_{s=-\infty}^{\infty} \left[\delta(i, I) \frac{z^s_{even}(I) - z(d_i)}{|z^s_{even}(I) - z(d_i)|^3} - \frac{z^s_{odd}(I) - z(d_i)}{|z^s_{odd}(I) - z(d_i)|^3} \cos(\theta_i) \right]; \quad \text{(A2)}$$

$$h_{I,CO} = a_{IC} \sum_{i=1}^{32} \sum_{s=-\infty}^{\infty} \left[\frac{1}{(z^s_{even}(I) - z(C_i))^2 + x(C_i)^2 + y(C_i)^2} - \frac{1}{(z^s_{odd}(I) - z(C_i))^2 + x(C_i)^2 + y(C_i)^2} \right] - (C_i \rightarrow O_i); \quad \text{(A3)}$$

$$h_{I,d'} = a_{I,d'} \sum_{s=-\infty}^{\infty} \left[\frac{\text{sign}(s)\delta(s, 0)}{|z^s_{even}(I) - z(d_i)|^2} - \frac{\text{sign}(2sL - 2z_I)}{|z^s_{odd}(I) - z(d_i)|^2} \right]; \quad \text{(A4)}$$

$$h_{d',CO} = a_{d',C}(\sin(\theta_I)\sin(\phi_I), \sin(\theta_I)\cos(\phi_I), \cos(\theta_I)) \quad \text{(A5)}$$

$$\cdot \sum_{i=1}^{32} \sum_{s=-\infty}^{\infty} \left[\frac{(x^{C,s}_{even} - x(I), y^{C,s}_{even} - y(I), z^{C,s}_{even} - z(I))}{[(z^{C,s}_{even} - z(I))^2 + (x^{C,s}_{even} - x(I))^2 + (y^{C,s}_{even} - y(I))^2]^{3/2}} - \frac{(x^{C,s}_{odd} - x(I), y^{C,s}_{odd} - y(I), z^{C,s}_{odd} - z(I))}{[(z^{C,s}_{odd} - z(I))^2 + (x^{C,s}_{odd} - x(I))^2 + (y^{C,s}_{odd} - y(I))^2]^{3/2}} \right]$$

$$+ (C \rightarrow O);$$

$$h_{d',D} = -a_{d',d} \sum_{k=1}^{32} \sum_{s=-\infty}^{\infty} \left[\frac{\Theta^-_{k,I}}{|z(I)^s_{even} - z(k)|^3} + \frac{\Theta^+_{k,I}}{|z(I)^s_{odd} - z(k)|^3} \right]; \quad \text{(A6)}$$

$$h_{d',d'} = a_{d',d'} \sum_{s=-\infty}^{\infty} \left[(3\cos^2(\theta_I) - 1) \frac{\delta(s, 0)}{|2sL|^3} + (\cos^2(\theta_I) + 1) \left| 2sL - 2z_I \right|^3 \right]. \quad \text{(A7)}$$

where

$$a_{Id} = kqp/\epsilon; \quad a_{IC} = kqq_C/\epsilon; \quad a_{I,d'} = k(1-k)qp/\epsilon; \quad \text{(A8)}$$

$$a_{d',C} = -(1-k)pq_C; \quad a_{d',D} = (1-k)p^2/\epsilon; \quad a_{d',d'} = (1-k)^2p^2/\epsilon; \quad \text{(A9)}$$

with

$$\Theta_{ij}^{\pm} = 2\cos(\theta_i)\cos(\theta_j) \pm \sin(\theta_i)\sin(\theta_j)\cos(\phi_i - \phi_j); \quad \text{(A10)}$$

$$\delta(k, m) = \begin{cases} 0 & \text{if } k = m, \\ 1 & \text{if } k \neq m. \end{cases} \quad \text{(A11)}$$

This work has been supported by grant GM-28643 from the National Institutes of Health.

REFERENCES

Åqvist, J., and A. Warshel. 1989. Energetics of ion permeation through membrane channels. Solvation of Na^+ by gramicidin A. *Biophys. J.* 56:171–182.

Andersen, O. S. 1983. Ion movement through gramicidin A channels. Single channel measurements at very high potentials. *Biophys. J.* 41: 119–133.

Andersen, O. S., and R. E. Koeppe. 1992. Molecular determinants of channel function. *Physiol. Rev.* 72:S89–S158.

Arseniev, A. S., V. F. Bystrov, T. V. Ivanov, and Y. A. Ovchinnikov. 1985. ^{1}H-nmr study of gramicidin A transmembrane ion channel. *FEBS Lett.* 186:168–174.

Becker, M. D., D. V. Greathouse, R. E. Koeppe II, and O. S. Andersen. 1991. Amino acid sequence modulation of gramicidin channel function. Effects of tryptophan-to-phenylalanine substitutions on the single-channel conductance and duration. *Biochemistry.* 30:8830–8839.

Beglov, D., and B. Roux. 1994. Finite representation of an infinite bulk system: solvent boundary potential for computer simulation. *J. Chem. Phys.* 100:9050–9063.

Berendsen, H., J. Grigera, and T. Straatsma. 1987. The missing term in effective pair potentials. *J. Phys. Chem.* 91:6269–6271.

Berendsen, H. J. C., J. P. M. Postma, W. F. van Gunsteren, and J. Hermans. 1981. Interaction models for water in relation to protein hydration. *In* Intermolecular Forces. B. Pullman, editor. Reidel, Dordrecht, the Netherlands. 331–342.

Binder, K., editor. 1979. Monte Carlo Methods in Statistical Physics. Springer-Verlag, Berlin, New York.

Bockris, J. O., and A. K. N. Reddy. 1977. Modern Electrochemistry. Plenum Press, Inc., New York.

Born, M. 1920. Volumen und Hydrationswarme der Ionen. *Z. Physik.* 1:45–48.

Buckingham, A. D. 1957. A theory of ion-solvent interaction. *Faraday Discuss. Chem. Soc.* 24:151–157.

Buehler, L. K., J. R. Granja, and M. R. Ghadiri. 1995. Permeation properties of self-assembling peptide nanotubes that form ion channels in planar lipid bilayers. *Biophys. J.* 65:A371.

Burgess, J. 1978. Metal ions in solutions. Horwood, Chichester, England.

Busath, D. D. 1993. The use of physical methods in determining gramicidin structure and function. *Ann. Rev. Physiol.* 55:473–501.

Chiu, S. W., E. Jakobsson, J. A. McCammon, and S. Subramaniam. 1989. Water and polypeptide conformation in the gramicidin channel. A molecular dynamics study. *Biophys. J.* 56:253–261.

Cieplak, P., T. P. Lybrand, and P. A. Kollman. 1987. Calculation of free energy changes in ion-water clusters using nonadditive potentials and the Monte Carlo method. *J. Chem. Phys.* 86:6393–6403.

Collins, K. D. 1995. Sticky ions in biological systems. *Proc. Nat. Acad. Sci. (U.S.A.).* 92:5553–5557.

Dani, J., and D. G. Levitt. 1981. Binding constants of Li, K and Tl in the gramicidin channel determined from water permeability measurements. *Biophys. J.* 35:485–500.

Durkin, J. T., L. L. Providence, R. E. Koeppe II, and O. S. Andersen. 1992. Formation of non-$\beta^{6.3}$-helical gramicidin channels between sequence substituted gramicidin analogues. *Biophys. J.* 62:145–159.

Eisenman, G. 1962. Cation selective glass electrodes and their mode of operation. *Biophys. J.* 2S:259–323.

Eisenman, G., and J. P. Sandblom. 1984. The pore dimensions of gramicidin A. *Biopys. J.* 45:88–90.

Elber, R., D. P. Chen, D. Rojewska, and R. Eisenberg. 1995. Sodium in gramicidin: an example of a permion. *Biophys. J.* 68:906–924.

Friedman, H. L., and C. V. Krishnan. 1973. Thermodynamics of ion hydration. *In* Water, a Comprehensive Treatis, Vol. 2. F. Franks, editor. Plenum, New York. 1–118.

Ghadiri, M. R., J. R. Granja, and L. K. Buehler. 1994. Artificial transmembrane ion channels from self-assembling peptide nanotubes. *Nature (Lond.).* 369:301–304.

Hille, B. 1992. Ionic Channels of Excitable Membranes. Sinauer Associates, Sunderland, MA.

Hirata, F., P. Redfern, and R. Levy. 1988. Viewing the born model for ion hydration through a microscope. *Int. J. Quantum Chem. Symp.* 15: 179–190.

Hol, W. 1985. The role of the α-helix dipole in protein function and structure. *Prog. Biophys. Mol. Biol.* 45:149–195.

Jakobsson, E., and S. W. Chiu. 1987. Stochastic theory of ion movement in channels with single ion occupancy. Application to sodium permeation of gramicidin channels. *Biophys. J.* 52:33–45.

Jayaram, B., B. Honig, K. A. Sharp, and R. Fine. 1989. Free-energy calculations of ion hydration. An analysis of the born model in terms of microscopic simulations. *J. Phys. Chem.* 93:4320–4327.

Jordan, P. C. 1979. Chemical Kinetics and Transport. Plenum Publishing Co., New York.

Jordan, P. C. 1984. The total electrostatic potential in a gramicidin channel. *J. Membr. Biol.* 78:91–102.

Jordan, P. C. 1990. Ion-water and ion-polypeptide correlations in a gramicidin-like channel. A molecular dynamics study. *Biophys. J.* 58: 1133–1156.

Jordan, P. C., J. A. McCammon, R. J. Bacquet, and P. Tran. 1989. How electrolyte shielding influences the electrical potential in transmembrane ion channels. *Biophys. J.* 55:1041–1052.

Jorgensen, W. L., R. W. Impey, J. Chandrasekhar, J. D. Madura, and M. L. Klein. 1983. Comparison of simple potential functions for simulating liquid water. *J. Chem. Phys.* 79:926–935.

Ketchem, R. R., W. Hu, and T. A. Cross. 1993. High resolution conformation of gramicidin A in a lipid bilayer by solid state NMR. *Science.* 261:1457–1460.

Kharkats, Y., and J. Ulstrup. 1991. The electrostatic gibbs energy of finite-size ions near a planar boundary between two dielectric media. *J. Electroanal. Chem.* 308:17–26.

Kienker, P. K., and J. D. Lear. 1995. Charge selectivity of the designed uncharged peptide ion channel Ac-$(LSSLLSL)_3$-$CONH_2$. *Biophys. J.* 68:1347–1358.

Killian, J. A. 1992. Gramicidin and gramicidin lipid interactions. *Biophys. Acta.* 1113:391–425.

Koeppe, R. E. and M. Kimura. 1984. Computer modeling of β-helical polypeptide models. *Biopolymers.* 23:23–38.

Koonin, S. E. 1986. Computational Physics. Benjamin-Cummings Pub. Co., New York.

Latimer, W. M., K. S. Pitzer, and C. M. Slansky. 1939. The free energy of hydration of gaseous ions, and the absolute potential of the normal calomel electrode. *J. Chem. Phys.* 7:108–111.

Lee, F. S., and A. Warshel. 1992. A local reaction field method for fast evaluation of long-range electrostatic interactions in molecular simulations. *J. Chem. Phys.* 97:3100–3107.

Lee, F. S., Z. T. Chu, and A. Warshel. 1993. Microscopic and semimicroscopic calculations of electrostatic energies in proteins by the POLARIS and ENZYMIX programs. *J. Comp. Chem.* 14:161–185.

Levitt, D. G. 1978. Electrostatic calculations for an ion channel. I: Energy and potential profiles and interaction between ions. *Biophys. J.* 22: 202–219.

Levitt, D. G. 1984. Kinetics of ion movement in narrow channels. *Curr. Top. Membr. Transp.* 21:181–197.

Liszi, J. and I. Ruff. 1985. Semi-microscopic models of ionic solvation. *In* The chemical physics of ionic solvation, Vol. 1. R. R. Dogonadze, E. Kalman, and A. A. Kornyshev, editors. Elsevier, Amsterdam. 119–142.

Mackay, D. H. J., P. H. Berens, A. T. Hagler, and K. R. Wilson. 1984. Structure and dynamics of ion transport through gramicidin A. *Biophys. J.* 46:229–248.

Marcus, Y. 1983. Thermodynamic functions of transfer of single ions from water to nonaqueous and mixed solvents. Part 1—Gibbs free energies of transfer to nonaqueous solvents. *Pure Appl. Chem.* 55:977–1021.

Marcus, Y. 1987. The thermodynamics of solvation of ions. Part 2.—The enthalpy of hydration at 298.15 K. *Faraday Soc. Trans.* 83:339–349.

Marcus, Y. 1991. Thermodynamics of solvation of ions. Part 5.—Gibbs free energy of hydration at 298.15 K. *Faraday Soc. Trans.* 87: 2995–2999.

Marcus, Y. 1994. A simple empirical model describing the thermodynamics of hydration of ions of widely varying charges, sizes, and shapes. *Biophys. Chem.* 51:111–127.

Mazet, J. L., O. S. Andersen, and R. E. Koeppe II 1984. Single-channel studies on linear gramicidins with altered amino acid sequences. A comparison of phenylalanine, tryptophan and tyrosine substitutions at positions 1 and 11. *Biophys. J.* 45:263–276.

Metropolis, N., A. W. Rosenbluth, M. N. Rosenbluth, A. H. Teller, and E. Teller. 1953. Equation of state calculations by fast computing machines. *J. Chem. Phys.* 21:1087–1092.

Monoi, H. 1991. Effective pore radius of the gramicidin channel. Electrostatic energies of ions calculated by a three dielectric model. *Biophys. J.* 59:786–794.

Nicholson, L. K., and T. A. Cross. 1989. Gramicidin cation channel. An experimental determination of the right-handed, single-stranded helix sense and verification of β-type hydrogen bonding. *Biochemistry.* 28: 9379–9385.

Noyes, R. M. 1962. Thermodynamics of ion hydration as a measure of effective dielectric properties of water. *J. Amer. Chem. Soc.* 84:513–522.

Noyes, R. M. 1964. Assignment of individual ionic contributions to properties of aqueous ions. *J. Amer. Chem. Soc.* 86:971–986.

Olah, G. A., H. W. Huang, W. Liu, and Y. Wu. 1991. Location of ion-binding sites in the gramicidin channel by X-ray diffraction. *J. Mol. Biol.* 218:847–858.

Pangali, C., M. Rao, and B. Berne. 1979. A Monte Carlo simulation of the hydrophobic interaction. *J. Chem. Phys.* 71:2975–2981.

Parsegian, V. A. 1969. Energy of an ion crossing a low dielectric membrane: solution of four relevant electrostatic problems. *Nature.* 221:844–846.

Parsons, R., editor. 1959. Handbook of electrochemical constants. Academic Press, New York.

Partenskii, M. B., and P. C. Jordan. 1992a. Nonlinear dielectric behavior of water in transmembrane ion channels: ion energy barriers and the channel dielectric constant. *J. Phys. Chem.* 96:3906–3910.

Partenskii, M. B., and P. C. Jordan. 1992b. Theoretical perspectives on ion-channel electrostatics: Continuum and microscopic approaches. *Q. Rev. Biophys.* 25:477–510.

Partenskii, M. B., M. Cai, and P. C. Jordan. 1991a. A dipolar chain model for the electrostatics of transmembrane ion channels. *Chem. Phys.* 153: 125–131.

Partenskii, M. B., M. Cai, and P. C. Jordan. 1991b. Influence of the pore-former charge distribution on the electrostatic properties of dipolar water chains in transmembrane ion channels. *Electrochim. Acta.* 36: 1753–1756.

Partenskii, M. B., V. Dorman, and P. C. Jordan. 1994. Influence of a channel-forming peptide on energy barriers to ion permeation, viewed from a continuum dielectric perspective. *Biophys. J.* 67:1429–1438.

Rashin, A. A., and B. Honig. 1985. Reevaluation of the born model of ion hydration. *J. Phys. Chem.* 89:5588–5593.

Rosenberg, P. A., and A. Finkelstein. 1978. Interaction of ions and water in gramicidin A channels. Streaming potentials across lipid bilayer membranes. *Biophys. J.* 27:455–460.

Roux, B., and M. Karplus. 1991. Ion transport in a model gramicidin channel. Structure and thermodynamics. *Biophys. J.* 59:961–981.

Roux, B., and M. Karplus. 1993. Ion transport in the gramicidin channel. Free energy of the solvated right-handed dimer in a model membrane. *J. Amer. Chem. Soc.* 115:3250–3262.

Roux, B., H. A. Yu, and M. Karplus. 1990. Molecular basis for the born model of ion solvation. *J. Phys. Chem.* 94:4683–4688.

Roux, B., B. Prod'hom, and M. Karplus. 1995. Ion transport in the gramicidin channel: molecular dynamics study of single and double occupancy. *Biophys. J.* 68:876–892.

Russell, E. W. B., L. B. Weiss, F. I. Navetta, R. E. Koeppe, II, and O. S. Andersen. 1986. Single-channel studies on linear gramicidins with altered amino acid side chains. Effects of altering the polarity of the side chain at position 1 in gramicidin a. *Biophys. J.* 49:673–686.

Sancho, M., M. B. Partenskii, V. Dorman, and P. C. Jordan. 1995. Extended dipolar chain model for ion channels: electrostriction effects and the translocation energy barrier. *Biophys. J.* 68:427–433.

Skerra, A., and J. Brickmann. 1987. Structure and dynamics of one-dimensional solutions in biological transmembrane channels. *Biophys. J.* 51:969–976.

Smart, O. S., J. M. Goodfellow, and B. A. Wallace. 1993. The pore dimensions of gramicidin A. *Biopys. J.* 65:2455–2460.

Straatsma, T. P., and H. J. C. Berendsen. 1988. Free energy of ionic hydration: analysis of a thermodynamic integration technique to evaluate free energy differences by molecular dynamics simulations. *J. Chem. Phys.* 89:5876–5886.

Sung, S. S., and P. C. Jordan. 1986. Structures and energetics of monovalent ion-water microclusters. *J. Chem. Phys.* 85:4045–4051.

Sung, S. S., and P. C. Jordan. 1987a. The interaction of Cl^- with a gramicidin-like channel. *Biophys. Chem.* 27:1–6.

Sung, S. S., and P. C. Jordan. 1987b. Why is gramicidin valence selective? A theoretical study. *Biophys. J.* 51:661–672.

Sung, S. S., and P. C. Jordan. 1988. Theoretical study of the antiparallel double-stranded helical dimer of gramicidin as an ion channel. *Biophys. J.* 54:519–526.

Urban, B. W., S. B. Hladky, and D. A. Haydon. 1980. Ion movements in gramicidin pores. An example of single-file transport. *Biochim. Biophys. Acta.* 602:331–354.

Urry, D. W., C. M. Venkatachalem, K. U. Prasad, R. J. Bradley, G. Parenti-Castelli, and G. Lenaz. 1981. Conduction processes of the gramicidin channel. *Int. J. Quant. Chem. Symp.* 8:385–399.

Verwey, E. J. W. 1942. The interaction of ion and solvent in aqueous solutions of electrolytes. *Recl. Trav. Chim. Pays-Bas, Belg.* 61:126–142.

Wada, A. 1976. The α-helix as an electric macro-dipole. *Adv. Biophys.* 9:1–63.

Wallace, B. A. 1990. Gramicidin channels and pores. *Annu. Rev. Biophys. Chem.* 19:127–157.

Wallace, B., and K. Ravikumar. 1988. The gramicidin pore: crystal structure of a cesium complex. *Science.* 241:182–187.

Warshel, A. 1979. Calculations of chemical processes in solution. *J. Phys. Chem.* 83:1640–1652.

Warshel, A., and S. T. Russell. 1984. Calculation of electrostatic interactions in biological systems and in solutions. *Q. Rev. Biophys.* 17:283–422.

Weiner, S. J., P. A. Kollman, D. A. Case, U. C. Singh, C. Ghio, G. Alagons, S. J. Profeta, and P. Weiner. 1984. A new force field for molecular mechanical simulation of nucleic acids and proteins. *J. Amer. Chem. Soc.* 106:756–784.